The interaction of microtubules with stabilizers characterized at biochemical and structural levels.

J. Fernando Díaz, José Manuel Andreu and Jesús Jiménez-Barbero

Centro de Investigaciones Biológicas, Consejo Superior de Investigaciones Científicas, Ramiro de Maeztu 9, 28040 Madrid, Spain.

E-mails: fer@cib.csic.es , j.m.andreu@cib.csic.es , jjbarbero@cib.csic.es

Table of Contents

3.5 Epothilones. Different geometries are found under different experimental conditions

3.6 Discodermolide and dictyostatin. The free and bound conformers

3.7 Peluroside A

Abstract.

Since the discovery of paclitaxel and its peculiar mechanism of cytotoxicity, which has made it and its analogues widely used antitumour drugs, a large effort has been done to understand the way they produce their effect in microtubules and to find other products that share this effect without their undesired side effects of (low solubility and development of multidrug resistance by tumour cells). This chapter reviews the actual knowledge about the biochemical and structural mechanisms of microtubule stabilization by microtubule stabilizing agents, and illustrates the way paclitaxel and its biomimetics induce microtubule assembly, the thermodynamics of their binding, the way they reach their binding site and the conformation they have when bound.

Keywords: Paclitaxel, Microtubule stabilizing agents, Antitumour drugs, Bioconformer.

Abbreviations: MSA, Microtubule stabilizing agent; Cr, critical concentration; GMPCPP, Guanosine-5'-[(α,β)-methyleno]triphosphate; PEDTA, 10 mM phosphate, 1 mM EDTA pH 6.7 buffer; RMSD, Root mean square deviation, NOE, Nuclear Overhauser Enhancement; REDOR, Rotational Echo Double Resonance; tr-NOE, transferred Nuclear Overhauser Enhancement; NOESY/STD, Nuclear Overhauser Enhancement spectroscopy/saturation transfer difference.

1. **Biochemical background on microtubule stabilizing agents.** What is a microtubule stabilizer?.

1.1 Microtubules and drugs

Small molecules modulating microtubule assembly have played major roles as tools for microtubule research, in a closely related manner to their chemotherapeutic interest [1]. Tubulin was first purified in the past century as the colchicine-binding protein proposed to be the subunit of cellular microtubules [2]. More recently, a colchicine derivative was employed to help crystallization and determine the structure of tubulin by X-ray diffraction [3]. The colchicine, vinblastine [4] and paclitaxel [5] sites are main drug binding sites of tubulin, to which many other substances bind. The discovery of microtubule stabilization by paclitaxel [6] prompted its clinical development [7] and a burst of research on new MSAs, as well as the generalized use of paclitaxel or docetaxel as convenient reagents to assemble (see Figure 1), stabilize or detect microtubules in the laboratory. One example is the development of the active fluorescent paclitaxel derivatives Flutax-1 and Flutax-2 [8] employed to study cellular microtubules [9] (see Figure 2) and as probes of the paclitaxel binding site [10], [11]. The electron crystallography determination of the structure of tubulin was made on two-dimensional tubulin crystals assembled with zinc and paclitaxel, providing the first atomic view of tubulin and bound paclitaxel [5] [12]. In this structure, tubulin forms protofilaments which associate in a different fashion from in a microtubule.

FIGURE 1.TIF

FIGURE 2.TIF

1.2 Function and evolution

It was speculated that the paclitaxel binding site of tubulin might bind an unknown endogenous regulator of microtubule assembly [6], but such a substance has never been documented so far. Therefore, we do not know whether the paclitaxel binding cavity has any physiological functions or is adventitiously formed as a result of microtubule assembly. The zones of microtubule associated proteins and motor proteins do not, in most cases, overlap the paclitaxel or other drug binding sites. Tubulin promiscuously binds a variety of exogenous small molecules, particularly from natural sources, some of which are plant poisons known since antiquity, which suggests that the production of microtubule poisons is an effective defensive mechanism against predators. Interestingly, a simpler relative of tubulin, bacterial cell division protein FtsZ [13], forms tubulin-like protofilaments which do not associate into microtubules [14] and does not bind most of these substances (JMA, unpublished), suggesting that the binding of antimitotic drugs by tubulin appeared with its ability to associate laterally into microtubules, or that plants and sponges have not developed a defensive mechanism targeting bacterial FtsZ.

1.3 What an MSA is and how it works.

A microtubule modulating molecule is, in a general thermodynamic definition, any ligand which binds to microtubules differently from unassembled tubulin. A ligand which preferentially binds to the unassembled protein will inhibit polymer formation, whereas a ligand which binds more to the polymers than to the unassembled protein will stabilize the polymers, due to

thermodynamic linkage [15]. This definition does imply neither knowledge of the site of binding nor of the changes in the structural dynamics of ligand and protein upon binding. Since from a structural point of view, a microtubule modulator may modify, either directly or allosterically, the polymerization interfaces of the tubulin molecule, one may obviously wish to know the mechanism by which such ligand modifies microtubule assembly, which requires kinetic and structural investigation. Structural modifications may in principle range from local side-chain rearrangements to significant domain movements, but translate in a few kcal per mol tubulin of microtubule stabilization. GTP is a natural cofactor which binds at the axial association interfaces between tubulin subunits [5],[16]. Several microtubule inhibitors are in a broad sense interfacial ligands [17] which bind like wedges at or near association interfaces between tubulin molecules [4] and therefore perturb their polymerization geometry to different extents. MSAs subtly modify microtubule structure. Paclitaxel, by binding near the lateral association interface between protofilaments, reduces the average number of protofilaments in microtubules made of purified tubulin from 13 to 12 [18], whereas its side-chain analogue docetaxel does not [19], and the fluorescent analogues Flutax-1 and Flutax-2 carrying a bulky fluorescent moiety increase the average number of protofilaments from 13 to 14 [10]. Finally, any substance that stabilizes cellular microtubules may be considered a MSA irrespective of its molecular target or mechanism.

1.4 Chemical diversity of MSAs in short

MSAs with different chemical structures have been discovered in different natural sources. Taxanes come from plants, epothilones and cyclostreptin are of microbial origin, whereas discodermolide, dictyostatin, eleutherobin, laulimalide and peloruside were discovered in sea organisms (for a classification and MSA structures see [20]). We do not know so far of MSAs with a purely synthetic chemistry not related to natural products.

1.5 Three MSA binding sites in microtubules

Many MSAs, including epothilones, discodermolide, dictyostatin, eleutherobin, sarcodictyin and a steroid derivative reversibly compete with taxanes to bind to the β-tubulin subunit in microtubules whereas cyclostreptin irreversibly inhibits taxane binding [20], [21], . Cyclostreptin binds covalently to a microtubule pore and to the lumenal taxoid binding site, indicating the entry pathway of taxanes into microtubules [20]. Binding to one site appears to exclude binding to the other, apparently because both sites use residues from the β-tubulin loop between helices H6 and H7 [22]. This opens the possibility that some MSAs may stop at the pore and not reach the lumenal site, as seems to be the case, at least partially, for fluorescent paclitaxel derivatives Flutax-2 and Hexaflutax [23]. On the other hand, laulimalide [24] and peloruside [25] share a binding site biochemically distinct from the paclitaxel site. Peloruside virtually docks into a zone of α-tubulin equivalent to that occupied by paclitaxel in β-tubulin [26], yet its binding site has not been experimentally located. We still do not know whether any more binding sites for stabilizing ligands may exist in microtubules.

1.6 Mechanisms and cellular consequences of microtubule stabilization.

Microtubule stabilizing agents at relatively high concentrations induce assembly of all tubulin available into microtubules, typically with accumulation of microtubule bundles in cells. The paclitaxel ligation of most tubulin molecules in a microtubule has interesting structural consequences, modifying microtubule flexural rigidity [27] and the curvature of dissociated protofilaments [28]. However, MSAs are active at lower concentrations at which they bind substoichiometrically to only a fraction of tubulin molecules in a microtubule. Under these substoichiometric conditions they suppress microtubule dynamic instability, a property in common with microtubule inhibitors, resulting in mitotic block or impairment, which eventually triggers tumour cell death [1] or senescence [29]. In addition, microtubule drugs can target tumour vasculature [1].

2. Thermodynamics and kinetic mechanisms of the interaction of stabilizing agents with microtubules. How do they bind?.

2.1 Thermodynamics of MSA induced microtubule assembly. How do they induce assembly?.

The main ability of microtubule stabilizing agents and the basis of their mechanism of action, is their capacity to induce microtubule assembly. Although different models ([30] [31]), based on the structure of the paclitaxel binding site [5], have been proposed to explain the paclitaxel mechanism of action on the basis of an structural effect on the tubulin molecule, it is unlikely, given the wide structural diversity of paclitaxel binding site ligands and the fact that there are at

least three different binding sites, (the internal and external paclitaxel sites and laulimalide one), that all of them produce the same structural effect at the atomic level on the microtubules.

On the other hand, from a thermodynamical point of view, a common mechanism for assembly induction can be proposed. All microtubule stabilizing agents bind tightly to the assembled form, while they do not apparently bind to the unassembled species [32], thus displacing the binding equilibrium towards the assembled form and so stabilizing them. Considering the difference in affinities for the assembled and unassembled species, it is straightforward to deduce that the compounds should displace the assembly equilibrium towards the polymerized form, as they fill the binding sites in microtubules.

However, preferential binding does not explain how microtubule assembly starts. Highly active microtubule stabilizing agents induce tubulin assembly in solution conditions in which no microtubules exist, and thus in which there is no equilibrium to be displaced [32],[20], implying that microtubule stabilizing agents have to bind unassembled tubulin to make it assemble into microtubules.

Microtubule assembly in the absence of ligands follows a non-covalent nucleated condensation polymerization, characterized by cooperative behaviour and by the presence of a critical concentration Cr, below which no significant formation of large polymers take place [32] (Figure 3). It can be demonstrated [33] that the apparent equilibrium constant for the growth reaction, i.e. the addition of a protomer to the polymer, is in good approximation, equal to the reciprocal critical concentration $Kp=Cr^{-1}$, which renders the apparent standard free energy change of elongation amenable to simple measurement (as long as

nucleotide hydrolysis is disregarded).

For ligand-induced assembly an apparent critical concentration, dependent on the ligand concentration, is observed [32]. Paclitaxel- and epothilone- induced assembly of GDP-tubulin have been extensively characterized. Under these conditions, in which tubulin is unable to assemble in the absence of ligand, assembly and binding are linked processes, there being no assembled unligated tubulin and showing an apparent critical concentration that saturates with ligand concentration (Figure 5 of [34] and Figure 2 of [35]), the latter not being compatible with a simple mechanism in which MSA stabilize microtubules binding to the empty sites in them.

FIGURE3.TIF

In principle, ligand induced tubulin assembly may proceed in two different ways [32], (Figure 4) the most intuitive one is the ligand-facilitated pathway (stabilization by binding to the empty sites, i.e. elongation precedes binding, Eq. 1, Figure 4A) i.e. the binding of a tubulin dimer creates a new high affinity binding site for the ligand, whose binding displaces the equilibrium towards the assembled form.

FIGURE4.TIF

$$Tub + Mtb \xleftrightarrow{Kel1} Tub - Mtb + Lig \xleftrightarrow{Kbin1} Tub - Mtb - Lig \quad (1)$$

Although this mechanism can not explain microtubule induced assembly in conditions in which tubulin is unable to assemble in absence of ligands, the ligand facilitated pathway is supported by the fact that paclitaxel does not bind unassembled tubulin (at least under non-assembly conditions), [32].

However, there is a strong argument against the ligand facilitated pathway: if the reaction proceeds via the ligand-facilitated pathway, the apparent elongation constant (the inverse of the dimer concentration in the supernatant) should depend linearly on the free concentration of ligand and its binding constant to the empty site (Equation 2).

$$Kel_{app} = Kel1 \cdot (1 + [Ligand] \cdot Kb1) \qquad (2)$$

This means that given two different ligands, at the same concentration, their power of assembly induction should depend linearly on the binding constant of the ligand, independently of the specific effect that the ligand causes on tubulin. Equation 2 predicts a continuous decrease of the critical concentration observed at overstoichiometric concentrations of microtubule stabilizing agents.

Apparently this is not the case. Although, in general, better binders are better assembly inductors, there are compounds that significantly deviate from the best regression line Figure 4A of [35], and Figure 4A [20], and a saturating behaviour of critical concentration with ligand concentration is observed (Figure 2 of [35] and Figure 5 of [34]).

This saturating behaviour observed is explained with both possible ligand-mediated pathways (binding precedes elongation), which are thermodynamically equivalent: a) the ligand binds to unassembled tubulin and the ligated dimer has a higher affinity for the microtubules, so decreasing the critical concentration (Eq. 3A, Figure 4B); b) the binding of a ligand to a non completed site at the end of the microtubule increases the affinity for the binding of the next dimer (Eq. 3B, Figure 4C).

$$Tub + Lig \xleftrightarrow{Kbin2} Tub - Lig + Mtb \xleftrightarrow{Kel2} Tub - Mtb - Lig \quad (3A)$$

$$Mtb + Lig \xleftrightarrow{Kbin2} Mtb - Lig + Tub \xleftrightarrow{Kel2} Tub - Mtb - Lig \quad (3B)$$

Mass action law predicts that if the ligand-mediated pathway were the only one that worked, the apparent critical concentration should saturate with the ligand concentration (equation 4), notwithstanding which of the pathways the reaction followed.

$$Kel_{app} = \frac{Kel2 \cdot Kbin2 \cdot [Ligand]}{(1 + Kbin2 \cdot [Ligand])} \quad (4)$$

So the critical concentration measured will depend on the elongation constant of the ligated dimer, which will depend on the specific effect that the ligand employed causes upon binding to a tubulin molecule.

However, since microtubule stabilizing agents will tightly bind to unoccupied sites, it is reasonable to assume that both mechanisms should work; but still in this case, the apparent critical concentration will saturate following equation (5):

$$Kel_{app} = Kel2 \cdot Kbin2 \frac{[Ligand] + \frac{1}{Kbin1}}{(1 + Kbin2 \cdot [Ligand])} \quad (5)$$

In practice, since at the paclitaxel or epothilone concentrations necessary to induce assembly, the concentrations of free ligand are of the order of 10^{-6} M, and $1/K_{bin1}$ for the strong assembly inducers is of the order of 10^{-7} to 10^{-9} M, the term $1/K_{bin1}$ can be neglected and so equation 5 becomes equivalent to eq. 4.

Following equations 4 or 5, it can be deduced that the measured Cr in saturation conditions (the experimental conditions) corresponds to the Cr of the ligated tubulin (or Cr of unligated tubulin to the ligated microtubule end) i.e. $1/K_{el2}$.

Although the ligand mediated pathways easily explain both the experimental results of assembly induction in conditions in which tubulin can not assemble in absence of the ligands and the saturation behaviour of Cr, it seems contradictory with the absence of observed binding of ligands to dimeric tubulin. Nevertheless, a first evidence of ligand binding to unassembled tubulin and to an alternative binding site in microtubules was obtained, supporting the hypothesis that the ligand mediated pathway is involved assembly induction by the microtubule stabilizing agents. Cyclostreptin, a covalent binding microtubule stabilizing agent of the paclitaxel site, [36], binds to the non assembled dimer [21] although with a slow kinetic rate in non-assembly conditions.

Thus, the most plausible hypothesis is that microtubule stabilizing agents induce microtubule assembly via a mechanism involving binding to unassembled tubulin dimers. Although microtubule stabilizing agents bind with high affinity to the empty sites in the microtubules, the equilibrium of the assembly process (the critical concentration) is determined by the change in the assembly properties of the dimer after binding to the microtubule stabilizing agent, and not by the binding affinity to the site itself.

2.2 Thermodynamics of MSA binding to microtubules. How to make them sticky?.

Microtubule stabilizing agents work because they bind microtubules. Improving this property is important for its action, since the better they bind to tubulin, the better cytotoxic agents they are [20, 35] [37]. In addition to this, high affinity or covalent microtubule stabilizing agents get trapped inside the cell due to the chemical potential of their interaction with tubulin, thus making escaping detoxification mechanism by membrane pumps overexpression, used by multidrug resistant cells [21],[37]

Early studies of the interaction between microtubule stabilizing agents with their binding sites were greatly hampered by the thermodynamics of ligand induced assembly [6]. [38]. Since microtubule stabilizing agents significantly perturb the assembly state of the protein, assembly and binding are linked processes and thus it is difficult to separate the contributions from both assembly and binding. It is thus, important to find conditions in which the assembly is not significantly perturbed due to the presence of the ligand.

Our first attempt to characterize the binding of paclitaxel and docetaxel to microtubules [34] was done at high concentrations of tubulin. Since in the conditions of the assay most of the tubulin gets assembled, the perturbation in the amount of assembled polymer is minimal, and a rigorous comparison between the binding affinity and the power of assembly induction of paclitaxel and docetaxel can be done. The study shows a single common binding site for paclitaxel and docetaxel for which docetaxel has double the affinity than paclitaxel (Figure 5). However it was not possible to measure directly the binding constant of paclitaxel and docetaxel. In order to do so, it would be

necessary to have empty assembled binding sites. Although empty sites can be assembled in the absence of ligand at high concentrations of tubulin, the high affinity observed for paclitaxel and docetaxel made it impossible to find conditions in which the reaction is not completely displaced towards the bound state.

FIGURE 5.TIF

The problem was overcome with the use of mildly fixed microtubules [10] in which the paclitaxel binding site is unaltered, while protected from cold and dilution depolymerisation. Using these stabilized microtubules, the binding constants of a paclitaxel molecule bound to a fluorescent probe (either fluorescein or difluorofluorescein) [8] was precisely determined and found to be of the order of $10^8 M^{-1}$ at 25ºC.

Having a fluorescent probe with a known binding site affinity, it was possible to design competition tests for the evaluation of the binding affinity of paclitaxel, docetaxel and bacatin III to microtubules, [11], [22] that can be used for fast and precise evaluation of a large series of compounds thus allowing precise studies of structure-affinity relationship [35] and to classify the microtubule stabilizing agents according to their binding sites [20], [24], [25].

The test has been used to measure the binding affinity of a set of 19 epothilones [35]. The study showed that it is possible to optimize the binding affinity of complex molecules by studding the effect of single changes in the substituents of the core of the molecule and combining the most favourable substitutions to obtain a 500 fold increase in the binding affinity of the epothilone molecule from Epothilone A (compound 1) to *cis*-CP-*tmt*-Epo B (compound 19) (Figure 6).

FIGURE 6.TIF

Moreover, the study demonstrates that the cytotoxicity of the compound on tumour cells is related to the binding affinity, being affinity of the compounds a variable to maximize in order to obtain more cytotoxic compounds.

The latter was generalized [20] for all paclitaxel binding site ligands known thus showing that the higher the affinity of the paclitaxel binding site the more cytotoxic the ligand.

From the equilibrium studies of microtubule stabilizing agents binding to the taxane site we learned the following: Microtubule stabilizing agents of the paclitaxel site bind microtubules with a well defined 1:1 stoichiometry. Binding affinity for a given fixed conformation of the molecule core can be modulated by selecting the side chain substituents with the highest contributions for the free energy of binding and combining them into a single molecule. The affinity of a compound is predictive of its cytotoxicity; thus it is possible to design more cytotoxic taxanes by studying the effect of each substitution on the binding affinity to select those which provide larger free energy changes to the binding.

2.3 Kinetics of MSA binding to microtubules. How do they reach their site in the microtubules?.

The kinetics of binding of ligands to a binding site provides information about the way the ligands reach the site. They may bind fast, indicating an easily accessible site, they may bind slowly indicating an occluded site. They may bind in a single step, indicating simple binding to a site or in successive steps, indicating a processing after early binding to a site.

One of the first effects of taxanes in microtubules observed was the fact that the structure of the paclitaxel-induced microtubules is different from that of the microtubules assembled in its absence [18]. Moreover, paclitaxel is able to change the structure of preformed docetaxel-induced assembled microtubules within a time range of the order of tens of seconds, indicating a fast exchange of taxanes in the site. [39]

The modification of the microtubule structure should come from the perturbation of the interprotofilament contacts, which allows the accommodation of extra protofilaments in the microtubule lattice. The experimental fact that taxane binding modifies the interprotofilament contacts rapidly leaded to the conclusion that the taxane binding site in microtubules was located in the interprotofilament space [18, 19].

The first structural location of the taxane binding site [40] placed it in the interprotofilament space, thus supporting the biochemical results. However, this changed when the first high resolution 3D structure of the paclitaxel-tubulin complex was solved by electron-crystallography of a two-dimensional zinc-induced tubulin polymer [5]. The fitting of this structure into a three-dimensional reconstruction of microtubules from cryoelectron microscopy allowed a pseudo atomic resolution model of microtubules [41] in which the paclitaxel binding site was placed inside the lumen of the microtubules hidden from the outer solvent.

The kinetics of taxane binding to microtubule were subsequently determined, taxanes and epothilones [10] [22, 23, 42] bind to microtubules extremely fast (Figure 7, Table I).

FIGURE 7.TIF

TABLE I

The binding of taxanes has been well characterized [10] [22] and shows a series of consecutive reactions involving a first fast bimolecular step (k_{+1} and k_{-1}), a second slow monomolecular step (k_{+2}, k_{-2}) and a third step which is the structural change involving the change in the number of microtubule protofilaments. It can be proved numerically that the first bimolecular fast step of binding is diffusion controlled, thus indicating that taxanes can not directly bind to the lumenal site [22].

Since the lumenal site of microtubules was well supported by the structural data and also by the fact that mutations in the lumenal site confer resistance to taxanes [43], an alternative mechanism with binding to an initial exposed binding site located in pore type one of the microtubule wall and later transportation of the ligand to the lumenal site was proposed in [22] (Figure 8).

FIGURE 8.TIF

The existence of the external site was further confirmed with a fluorescein-tagged taxane, Hexaflutax, specially tailored with an spacer between the taxane moiety and the fluorescein tag, long enough to allow binding to an external site while keeping the fluorescent tag exposed to an antibody but short enough to avoid antibody binding if the taxane moiety is bound to the lumenal site. It was shown that monoclonal and polyclonal antibodies bind to Hexaflutax bound to microtubules at a kinetic rate consistent with a diffusion controlled bimolecular reaction between two objects of the size of a microtubule and an antibody, forming an stable ternary complex, thus indicating that at least a significant part of the taxane is bound to an external site [23].

FIGURE 9.TIF

The route of taxanes was finally unveiled with the use of a covalent ligand of the taxane binding site [21]. Cyclostreptin, a bacterial natural product [44] [45] with weak, but irreversible tubulin assembly activity and strong apparent binding affinity for the paclitaxel site, covalently labels both a residue placed in the lumenal site of paclitaxel Asn228 and a residue previously proposed to be in the external binding site Thr220 (Figure 9A).

From these results a structural binding pathway consistent with that observed kinetically was proposed [21]. Paclitaxel binds fast to a site located in the surface of the microtubules, into the type 1 pore. Then, it has to be transferred to the second luminal, final location. The transfer involves probably the switch of some of the elements of the first site, since only one molecule of paclitaxel can bind to each molecule of β-tubulin (Figure 9B).

The kinetic information can be used as well to deduce if a compound is bound homogeneously or not, from the kinetic data known Flutax, and paclitaxel dissociation from β-tubulin is monophasic, which indicates a single rate limiting step, consistent with most of the compound bound to the same site. However, dissociation of Epothilone A from the binding site shows biphasic behaviour, which would be consistent with the compound distributed between the external and the luminal site, with a temperature-dependant equilibrium (Table II).

INSERT TABLE 2

From the kinetics of ligand binding to microtubules we can obtain valuable information about the way paclitaxel microtubule stabilizing agents reach their binding site. They bind to an external binding site located in the pores of the microtubule wall from which they are totally or partially relocated to an inner luminal site.

3. The bioactive conformations of MSA. How do they look like when bound?.

Many attempts have been made over the last years to deduce the actual pharmacophore/s for the recognition of MSA by microtubules. For newly designed MSA to serve as effective anticancer drugs, it seems reasonable that they should be able to achieve a conformation compatible with the binding pocket of the target protein. On this basis, many scientists have focused on determining the bioactive conformation of the different MSAs.

3.1 Paclitaxel and related molecules. The single conformer hypothesis

The study of the tubulin-bound conformation of paclitaxel has resulted in a number of protein-ligand models, partially or fully based on the electron diffraction structure of $\alpha\beta$-tubulin in paclitaxel-stabilized Zn^{+2}-induced sheets. [12] [5]. Obviously, the nature of the paclitaxel binding site and the paclitaxel conformation in the binding site have key implications for the design of new MSA. A deep knowledge of the bioactive conformation would also help to explain how compounds as structurally diverse as the epothilones, [46] discodermolide, [47] and eleutherobin [48] have very similar mechanisms of action.

After the first photoaffinity labelling studies, which were the first methods used to define the paclitaxel binding site on tubulin, and indeed allowed identifying different amino acids of β-tubulin as putative parts of the binding site, [49] the initial efforts to correlate activity (or binding) with the solid state, solution or modelled conformations of MSA in their free states lead to the first pharmacophore proposals. [50] At first, the existence of only a very limited set

of conformations for these molecules was assumed, [51] while more recently, it was considered that most of these molecules are intrinsically flexible and may assume a variety of shapes [52].

Previous investigations on this topic until the beginning of 2002 have been already reviewed, [53] further expanded more recently, [54] gathering the knowledge of the conformation of these molecules under different conditions. Until 2001, also corresponding to the availability of the αβ-tubulin coordinates from the electron crystallography structure [5],[12] the attempts to codify the bound conformation of MSA were derived from ligand conformations acquired in the free state by either X-ray crystallography or NMR studies. An assumed or modelled bioactive form was then employed as a template for superimposition by other ligands to try to deduce the pharmacophore [55].

After the availability of the 3.7 Å resolution electron crystallographic structure of paclitaxel bound to αβ-tubulin, [5] further refined at 3.5 Å resolution [12] different research groups tried to probe the binding conformation of MSA at the key β-subunit. Nevertheless, although paclitaxel indeed stabilized the actual microtubule sheets examined by electron crystallography. The first coordinates of tubulin deposited (1TUB) contained the single crystal coordinates for docetaxel [56] instead of the actual ligand, due to problems to fully characterize either the binding mode or the conformation of bound paclitaxel. On this basis, only qualitative statements could first be made concerning the details of ligand binding. Nonetheless, the location of the drug was consistent with the former photoaffinity labelling results and showed that paclitaxel occupies a hydrophobic cleft on β-tubulin. Furthermore, the ligand density suggested that one of the phenyl rings at the C-3' terminus was near the top of helix H1, while the C-2

benzoyl moiety was close to H5 and to the H5-H6 loop. In the refined structure (1JFF), [12] the taxane ring was better defined, but the densities for both the 2-phenyl side-chain and the N'-phenyl group still remained low, suggesting certain mobility of these groups. Nevertheless, according to the authors, the refined paclitaxel structure adopted a geometry very similar to that determined independently by energy-based refinement [57], except for the key torsional rotations of the side-chain phenyl rings. We will turn back to this point below.

Before these investigations, most of the models of the paclitaxel-tubulin interaction had been directly extrapolated from the conformations of paclitaxel found either in polar [58] or non-polar media [59] and from the single crystal X-ray structure of docetaxel (Figure 10). [56]

FIGURE 10.TIF

3.2 Paclitaxel and related molecules. Flexibility

Indeed, before 2000, single conformers had been basically considered, although it was possible that the multiple torsional degrees of freedom of these molecules would produce a complex multidimensional energy surface, and therefore, a variety of putative 3D geometries capable of interacting with the tubulin binding site. [60],[61]. Numerous research teams pursued different indirect approaches to the pharmacophore determination. The first and earliest attempts relied on studies of the structure-activity relationship of the taxane skeleton [62] [50], [51], [52], which included quantitative calculations [51]. These studies demonstrated that the presence and the spatial disposition of the three flexible side chains at C-4, C-2 and C-13 defined the conformations proposed or

determined in both solution, in the solid state and at the β-tubulin binding site, since the baccatin core (A-D rings) was conformationally well-defined [63].

A more complete structure-based approach used (bio-)physical methods, in particular X-ray, NMR spectroscopy and/or molecular modelling, to study the structure and conformations of paclitaxel in its uncomplexed state, trying to extrapolate these findings to the bound form. Single crystal X-ray analysis in the solid state defined different conformers for different analogues, [64] while NMR analysis in polar and non-polar media indeed identified others. [65], [66], [67], [68], [69], [70],[71]. In all cases, these reports assumed a major single conformation, although later, Snyder's group, through deconvolution of the NMR data obtained for paclitaxel in $CDCl_3$ [60] and D_2O/DMSO-d_6 (Snyder JP, Nevins, N, Jímenez-Barbero, J, Cicero, D and Jansen JM, unpublished) solutions identified many (9–10) conformations in these solvents, none of them showing a population above 30%. Nevertheless, the structural details from NMR were interpreted in terms of the key features of the dominant conformations: the NOE data in polar solvents showed that, to some extent, the C-3' phenyl group is hydrophobically collapsed with the C-2 benzoyl phenyl (the "polar" conformer, Figure 11), while in non-polar solvents the data evidenced an analogous phenyl-phenyl association between the C-3' benzamido phenyl and the one at the terminus of the C-2 side chain (the "nonpolar" conformer) [50], [51], [52], [55], [72], [73]. As previously reviewed, [53] both the polar and the nonpolar conformations were proposed as the bioactive forms. It was also speculated that an eclipsed conformer related to the polar form could be the one recognized by the tubulin binding site [73].

FIGURE 11.TIF

3.3 Synthetic analogues. The quest for the actual bioactive geometry

These interpretations prompted many organic chemists to prepare synthetic analogues, bridging different regions of the paclitaxel molecule, aimed at locking or at least favouring the putative bioactive conformation of paclitaxel on tubulin (see below for further discussion). [74], [54] A large discussion and controversy among different groups has been established on the bioactive three-dimensional form of paclitaxel. In a first REDOR NMR study, F-^{13}C distances between the fluorine of a 2-(*p*-fluorobenzoyl) paclitaxel and both the C-3' amide carbonyl and C-3' methine carbons were estimated, [75] permitting a serious attempt to determine key aspects of the ligand conformation at the β-tubulin binding site [76]. Complementary measurements of fluorescence-resonance energy transfer suggested a model for the paclitaxel binding mode. In a second study, a distance of 6.5 Å was determined between the fluorine atoms of 2-(*p*-fluorobenzoyl)-3'-(*p*-fluorophenyl)-10-acetyl-docetaxel [77]. Recent studies using a variety of fluorinated and deuterated analogues, also using REDOR [78] have led the authors of this investigation to conclude that the bound form is in agreement with the so-called T-Taxol geometry (see below), [57] [79] and not with other REDOR-based geometry proposed by other research group, dubbing New York (NY-Taxol) [76].

3.4 The T-Taxol conformer

Computational studies have been of paramount importance in order to integrate the results of the experimental studies indicated above with the electron crystallographic data known. According to Snyder and co-workers, a satisfactory and experimentally verifiable model of the tubulin-binding site and

of the conformation of paclitaxel has been obtained by computational methods on the first electron crystallographic model. In this context, a new paclitaxel conformer, T-Taxol (Figure 12), has been proposed [57], [79], [80].

FIGURE 12.TIF

Further refinement of the electron crystallographic structure of tubulin-paclitaxel at 3.5 Å resolution delivered a similar result. Nevertheless, the T-Taxol model has not been completely accepted as the actual bioactive conformation [76]. It is evident that the low 3.5–3.7 Å resolution of the complex limits the precision of the resulting model. In addition, the Zn^{2+}-stabilized tubulin preparation employed in the electron crystallographic study involves antiparallel protofilaments organized in sheets, which strongly differ from genuine microtubules. Consequently, concern has been expressed that the sheets may not be representative of cellular microtubules and that sheet-bound paclitaxel geometry may differ from its bioactive form in microtubules.

In this context, using the different models as templates, different synthetic organic chemistry groups have prepared cyclic, conformationally-constrained analogues based on the T-Taxol structure, leading to molecules with potencies similar or even greater than the lead structure. [54], [74], [76] [81]. Different research groups have introduced constraints into the paclitaxel molecule involving the C-4, C-2 and C-13 side chains. Interestingly, it has been reported that forming a tether between the C-4 acetate methyl and the *ortho*-center of the C-3' phenyl, in agreement with the proposed T-Taxol conformation, permits the access to compounds with much better activities (three, thirty or fifty-fold) than the activity of paclitaxel, even when tested against both paclitaxel- and epothilone-resistant cell lines. It has been proposed that the

origin of the bioactivities is related to the degree of rigidification introduced by the C-4 to C-3' bridging moieties. While for paclitaxel, the T-form was estimated to be present in only 2-5% of the variety of conformations, [57], [81] the key constrained compounds appeared with 76% and 86% contributions from T-Taxol-like geometries. Nevertheless, the authors have also warned that the significant activity increases measured for these substances could not be attributed completely to conformational biasing, although it seems to be a dominating factor. Indeed, they proposed that reinforcing the T-Taxol conformation is a necessary but not sufficient condition to elicit high levels of drug potency. [81] Especially, in addition to the appropriate molecular conformation, the ligand must also show a tubulin-compatible molecular volume.

3.5 Epothilones. Different geometries are found under different experimental conditions

As for all MSAs, the investigation of the complex of epothilones [55] with microtubules has also been attempted. The solid state (deduced by either X-ray or solid state NMR) structure of free epothilone B is known, as well as its solution conformations [82] [83]. However, its actual bioactive conformation is also a matter of debate.

For the free state, the major conformation of the macrocycle in solution is similar to that found in the crystal, although there was no preferred conformation of the thiazole side chain, which showed a substantial freedom of the side chain around the C17-C18 bond.

In contrast, approach to the structure determination by solid-state NMR, [84] has proposed a more defined geometry of both the macrocycle and the side chain. In fact, the ten solid-state NMR structures derived were very well defined, while the average RMSD of the heavy atom to the X-ray structure was only 0.75 Å. When comparing assignments of the solid-state NMR with the previously reported solution-state NMR data, [82] a qualitative correlation was found between the chemical-shift variations observed and the possibility of intermolecular hydrogen-bonding [84].

The first study of the bioactive conformation of epothilones was conducted through solution-state NMR for epothilone A, which lacks the methyl group at C12, bound to non-microtubule assembled $\alpha\beta$-tubulin. [85] [86] Almost immediately, the tubulin/epothilone A complex was studied through electron-crystallography for Zn^{2+}-stabilized $\alpha\beta$-tubulin layers. [87] The conformation of the tubulin-bound epothilone was strikingly different in the two studies, suggesting the need for further investigation. As this discrepancy may reflect the dependence of the epothilone binding mode on the tubulin polymerization state, further studies are still expected.

From the viewpoint of NMR, the existence of specific and transient binding of epothilone A to tubulin enabled the structural analysis of the active conformation [85] [86] of the epothilones by using trNOESY experiments, in particular, using the interligand NOE for pharmacophore mapping (INPHARMA) methodology [88] and molecular modeling.

For the NMR structural investigation of the epothilone-tubulin complex in solution, microtubule assembly was prevented. Evident conformational differences were observed between the X-ray crystal structure and the tubulin-

bound NMR conformation of epothilone A. However, the authors rationalized many structure-activity relationship data available on the tubulin-polymerization activity of several epothilone derivatives [89]. According to these authors, the electron crystallography-derived model [87] of the epothilone A-tubulin complex did not support some of the structure activity relationship data. Nevertheless, as also stated in [88], the high flexibility of the M loop, the S9-S10 loop, and the H6-H7 loop forming the binding pocket could be responsible for different binding modes of epothilone A to tubulin, depending on the polymerization state.

Although according to the NMR analysis in non-polar solvents [82], the most populated conformer is indeed very similar to the X-ray conformer, evidences of other conformers are also clearly observed in the NMR data in solution for the free state. The comparison of the torsion angles of epothilone A in the tubulin-bound and in the free conformation revealed two major changes: the first occurred in the O1-C6 region, while the second affected the orientation of the thiazole ring respect to the C16-C17 double bond. Neither the C6-C7 dihedral angle, nor the C10-C15 region exhibited significant conformational changes upon binding to tubulin. The most significant difference between the free and tubulin-bound conformations of epothilone occurred in the side chain with the thiazole ring. In the geometry of the bound conformation, the nitrogen atom of the thiazole ring becomes more accessible for potential formation of hydrogen bonds with the protein, which may more than offset the deduced high-energy epothilone side-chain conformation. The design of epothilone analogues should now use the knowledge about the conformation of epothilone in its tubulin-bound state.

3.6 Discodermolide and dictyostatin. The free and bound conformers

An elegant recent work by Carlomagno et al. [90], has reported the unassembled-tubulin-bound conformation of discodermolide. Nevertheless, since the taxane binding site does not exist for unassembled tubulin [32] [21], it is unlikely that the tubulin-bound conformation observed therein [90] is the conformation bound to the luminal taxane binding site, but most likely to the external site. Nevertheless, under these experimental conditions, the tubulin-bound conformation of discodermolide in solution from NMR tr-NOE data is a compact globular shape. With the help of both protein-mediated interligand NOE signals between discodermolide and Epothilone [90] and the SAR data available for the two drugs, a common pharmacophore model was proposed. Similarities and differences in the pharmacophore of the two drugs may provide a rationale for the analogous but not fully equivalent biological activities of the two natural products. Also, the similarity between the tubulin-bound conformation of discodermolide and its X-ray structure [91] provides a rationale for the powerful biological activity of the marine natural product dictyostatin, a 22-membered macrocyclic lactone which is structurally and biogenetically related to discodermolide. Not surprisingly, the tubulin-bound conformation of discodermolide derived therein [90] was closely related to the solution structure of dictyostatin, [92] which supports a common mechanism for the MT-stabilizing activity of the two compounds.

A variety of NMR data, including trNOESY/STD and line broadening analysis, and using also NMR competition experiments, assisted by molecular mechanics calculations, has also been recently employed to deduce the microtubule-bound conformation of the previously mentioned two MSA,

discodermolide and dictyostatin [93] Since it is well known that tubulin in plain phosphate buffer does not assemble into microtubules, and it has been described that the microtubule taxoid binding site does not exist in dimeric tubulin, at least with an affinity higher than millimolar, we rather preferred to search for biochemical conditions in which stable microtubules were assembled from native tubulin with GMPCPP [26]. The NMR data obtained indicated that microtubules recognize discodermolide through a conformational selection process, in which the half-chair conformer (and not the predominant in water solution, skew boat form) of the lactone moiety is bound by the receptor. There are minor changes in the rest of the molecular skeleton between the major conformer in water solution and that bound to assembled microtubules. Indeed, despite the many torsional degrees of freedom of discodermolide, intramolecular interactions within the molecule and hydration strongly affects its conformational features, which indeed only shows conformational mobility around a fairly narrow part of the molecule. This evidence contrasts strongly with the observations on other solvents, in which discodermolide shows different degrees of flexibility. Therefore, while in acetonitrile [94] or dimethyl sulfoxide, [95] the different torsional degrees of freedom of discodermolide show different flexibilities, the orientation of the C5-C24 chain is highly pre-organized in water solution [93] respect to that bound by tubulin, probably to minimize entropic penalties. There are some slight changes in the deduced microtubules-bound conformation respect to that described by Carlomagno et al. using non-assembled tubulin. (Fig. 13) The structure provided by Carlomagno et al. [90] shows a chair for the six-membered ring and its orientation is different from the rest of the chain. Very probably, this slight

discrepancy is due to the different employed force fields by the two groups. In any case, the presentation of the molecule is remarkably similar, despite the change in the mode of preparation of tubulin in the two cases. Specially, van der Waals contacts and torsional constraints strongly bias its conformational behaviour. Yet, this feature serves to modulate the presentation of polar and non-polar surfaces to interact with the binding site of tubulin. A model of the binding mode of discodermolide to tubulin has also been proposed, involving the β-tubulin monomer by using docking simulations [93]. This model involves the taxane binding site of tubulin and comprises both polar and non polar interactions between discodermolide and the receptor.

FIGURE 13.TIF

The microtubule-bound conformation of an analogous MSA, dictyostatin, has also been derived by using the same combined protocol of NMR spectroscopy and molecular docking. [93] The bound geometry deduced (Fig. 14) presents some key conformational differences against the major one existing in solution [96] around torsion angles at the C-7 region, and additionally displays mobility (even when bound) along the lateral C22-C26 chain. In any case, the bound conformer of dictyostatin resembles that of discodermolide and provides very similar contacts with the receptor. Competition experiments have indicated that both molecules compete with the taxane-binding site, providing further support to previously described biochemical data.

FIGURE 14.TIF

3.7 Peluroside A

The conformation of Peluroside A bound to microtubules has also been investigated. Two low energy conformations of Peloruside A have been found in water solution, [26] which mainly differ in the relative orientation of the C10 to C15 region (Figure 15). One of these geometries (A) is in agreement with that postulated for Peloruside A in chloroform solution. [97] [98] From viewpoint of energy, and using MM3*, the new conformer (B) is more stable than A. The major energy component that stabilizes B is solvation energy. Nevertheless, according to molecular dynamics simulations, both conformers are flexible along the backbone, with somehow higher variations for the lateral chain. Nevertheless, despite the large size of the macrocyclic ring, intramolecular interactions (van der Waals contacts and torsional constraints) within the Peloruside A ring strongly affect the conformational features of this molecule, which indeed only shows conformational mobility around a fairly narrow part of the molecule. Yet, this existing conformational freedom, in the presence of a given solvent, serves to modulate the presentation of polar and nonpolar surfaces to interact with the binding site.

FIGURE 15.TIF

In the bound state, the NMR data, assisted by molecular mechanics calculations and docking experiments, indicated that only one (that present in water, B) of the two major conformations existing in water solution is bound to microtubules (α-tubulin). A model of the binding mode to tubulin has also been proposed, [26] involving the α-tubulin monomer, in contrast with paclitaxel, which binds to the β-monomer.

It can be expected that the near future will provide tubulin-ligand structures with sufficient accuracy to define precisely the conformation and binding mode for these compounds and thereby validate or reject the current set of models. For the time being, the methodologies schematically reviewed here may provide additional data for understanding the action of MSAs and hopefully to design new potent analogues.

References

1. Jordan MA, Wilson L (2004) Nat Rev Cancer 4: 253
2. Weisenberg RC, Borisy GG, Taylor EW (1968) Biochemistry 7: 4466
3. Ravelli RB, Gigant B, Curmi PA, Jourdain I, Lachkar S, Sobel A, Knossow M (2004) Nature 428: 198
4. Gigant B, Wang C, Ravelli RB, Roussi F, Steinmetz MO, Curmi PA, Sobel A, Knossow M (2005) Nature 435: 519
5. Nogales E, Wolf SG, Downing KH (1998) Nature 391: 199
6. Schiff PB, Fant J, Horwitz SB (1979) Nature 277: 665
7. Wall ME, Wani MC (1995) Cancer Res 55: 753
8. Souto AA, Acuna AU, Andreu JM, Barasoain I, Abal M, AmatGuerri F (1996) Angew Chem Int Ed Engl 34: 2710
9. Evangelio JA, Abal M, Barasoain I, Souto AA, Lillo MP, Acuna AU, Amat-Guerri F, Andreu JM (1998) Cell Motil Cytoskeleton 39: 73
10. Diaz JF, Strobe R, Engelborghs Y, Souto AA, Andreu JM (2000) J Biol Chem 275: 26265
11. Andreu JM, Barasoain I (2001) Biochemistry 40: 11975
12. Lowe J, Li H, Downing KH, Nogales E (2001) J Mol Biol 313: 1045

13. Lowe J, Amos LA (1998) Nature 391: 203

14. Huecas S, Llorca O, Boskovic J, Martín-Benito J, Valpuesta JM, Andreu JM (2007) Biophys J doi:10.1529/biophysj.107.115493

15. Wyman J, Gill SJ (1990) Binding and linkage. University Science Books, Mill Valley, Ca

16. Menendez M, Rivas G, Diaz JF, Andreu JM (1998) J Biol Chem 273: 167

17. Pommier Y, Cherfils J (2005) Trends Pharmacol Sci 26: 138

18. Andreu JM, Bordas J, Diaz JF, Garcia de Ancos J, Gil R, Medrano FJ, Nogales E, Pantos E, Towns-Andrews E (1992) J Mol Biol 226: 169

19. Andreu JM, Diaz JF, Gil R, de Pereda JM, Garcia de Lacoba M, Peyrot V, Briand C, Towns-Andrews E, Bordas J (1994) J Biol Chem 269: 31785

20. Buey RM, Barasoain I, Jackson E, Meyer A, Giannakakou P, Paterson I, Mooberry S, Andreu JM, Diaz JF (2005) Chem Biol 12: 1269

21. Buey RM, Calvo E, Barasoain I, Pineda O, Edler MC, Matesanz R, Cerezo G, Vanderwal CD, Day BW, Sorensen EJ, Lopez JA, Andreu JM, Hamel E, Diaz JF (2007) Nat Chem Biol 3: 117

22. Diaz JF, Barasoain I, Andreu JM (2003) J Biol Chem 278: 8407

23. Diaz JF, Barasoain I, Souto AA, Amat-Guerri F, Andreu JM (2005) J Biol Chem 280: 3928

24. Pryor DE, O'Brate A, Bilcer G, Diaz JF, Wang Y, Kabaki M, Jung MK, Andreu JM, Ghosh AK, Giannakakou P, Hamel E (2002) Biochemistry 41: 9109

25. Gaitanos TN, Buey RM, Diaz JF, Northcote PT, Teesdale-Spittle P, Andreu JM, Miller JH (2004) Cancer Res 64: 5063

26. Jimenez-Barbero J, Canales A, Northcote PT, Buey RM, Andreu JM, Diaz JF (2006) J Am Chem Soc 128: 8757

27. Dye RB, Fink SP, Williams RC (1993) J Biol Chem 268: 6847

28. Elie-Caille C, Severin F, Helenius J, Howard J, Muller DJ, Hyman AA (2007) Current Biology 17: 1765

29. Klein LE, Freeze BS, Smith AB, Horwitz SB (2005) Cell Cycle 4: 501

30. Amos LA, Lowe J (1999) Chem Biol 6: R65

31. Li H, DeRosier DJ, Nicholson WV, Nogales E, Downing KH (2002) Structure (Camb) 10: 1317

32. Diaz JF, Menendez M, Andreu JM (1993) Biochemistry 32: 10067

33. Oosawa F, Asakura S (1975) Thermodynamics of the polymerization of protein,. Academic Press, London

34. Diaz JF, Andreu JM (1993) Biochemistry 32: 2747

35. Buey RM, Diaz JF, Andreu JM, O'Brate A, Giannakakou P, Nicolaou KC, Sasmal PK, Ritzen A, Namoto K (2004) Chem Biol 11: 225

36. Edler MC, Buey RM, Gussio R, Marcus AI, Vanderwal CD, Sorensen EJ, Diaz JF, Giannakakou P, Hamel E (2005) Biochemistry 44: 11525

37. Yang C, Barasoain I, Li X, Matesanz R, Liu R, Sharom FJ, Diaz JF, Fang W (2007) Chem Med Chem 2: 691

38. Schiff PB, Horwitz SB (1981) Biochemistry 20: 3247

39. Diaz JF, Valpuesta JM, Chacon P, Diakun G, Andreu JM (1998) J Biol Chem 273: 33803

40. Nogales E, Wolf SG, Khan IA, Luduena RF, Downing KH (1995) Nature 375: 424

41. Nogales E, Whittaker M, Milligan RA, Downing KH (1999) Cell 96: 79

42. Díaz JF, Buey RM (2007) In: Zhou J (ed) Methods in Molecular Medicine, vol 137. Humana Press Inc., Totowa, NJ p 245

43. Giannakakou P, Sackett DL, Kang YK, Zhan Z, Buters JT, Fojo T, Poruchynsky MS (1997) J Biol Chem 272: 17118

44. Sato B, Muramatsu H, Miyauchi M, Hori Y, Takase S, Hino M, Hashimoto S, Terano H (2000) J Antibiot (Tokyo) 53: 123

45. Sato B, Nakajima H, Hori Y, Hino M, Hashimoto S, Terano H (2000) J Antibiot (Tokyo) 53: 204

46. Nicolaou KC, Roschangar F, Vourloumis D (1998) Angew Chem Int Ed Engl 37: 2015

47. Kalesse M (2000) Chembiochem 1: 171

48. Lindel T, Jensen PR, Fenical W, Long BH, Casazza AM, Carboni J, Fairchild CR (1997) J Am Chem Soc 119: 8744

49. Rao S, He LF, Chakravarty S, Ojima I, Orr GA, Horwitz SB (1999) J Biol Chem 274: 37990

50. Czaplinski KHA, Grunewald GL (1994) Bioorg Med Chem Lett 4: 2211

51. Morita H, Gonda A, Wei L, Takeya K, Itokawa H (1997) Bioorg Med Chem Lett 7: 2387

52. Wang M, Xia X, Kim Y, Hwang D, Jansen JM, Botta M, Liotta DC, Snyder JP (1999) Org Lett 1: 43

53. Jimenez-Barbero J, Amat-Guerri F, Snyder JP (2002) Curr Med Chem Anti-Canc Agents 2: 91

54. Kingston DGI, Bane S, Snyder JP (2005) Cell Cycle 4: 279

55. Giannakakou P, Gussio R, Nogales E, Downing KH, Zaharevitz D, Bollbuck B, Poy G, Sackett D, Nicolaou KC, Fojo T (2000) Proc Natl Acad Sci U S A 97: 2904

56. Gueritte-Voegelein F, Guenard D, Mangatal L, Potier P, Guilhem J, Cesario M, Pascard C (1990) Acta Cryst C 46: 781

57. Snyder JP, Nettles JH, Cornett B, Downing KH, Nogales E (2001) Proc Natl Acad Sci U S A 98: 5312

58. Vandervelde DG, Georg GI, Grunewald GL, Gunn GW, Mitscher LA (1993) J Am Chem Soc 115: 11650

59. Williams HJ, Scott AI, Dieden RA, Swindell CS, Chirlian LE, Francl MM, Heerding JM, Krauss NE (1994) Can J Chem 72: 252

60. Snyder JP, Nevins N, Cicero DO, Jasen J (2000) J Am Chem Soc 122: 724

61. Johnson SA, Alcaraz AA, Snyder JP (2005) Org Lett 7: 5549

62. Zhu QQ, Guo ZR, Huang N, Wang MM, Chu FM (1997) J Med Chem 40: 4319

63. Moyna G, Williams HJ, Scott AI, Ringel I, Gorodetsky R, Swindell CS (1997) J Med Chem 40: 3305

64. Mastropaolo D, Camerman A, Luo YG, Brayer GD, Camerman N (1995) Proc Natl Acad Sci U S A 92: 6920

65. Gomez Paloma L, Guy RK, Wrasidlo W, Nicolaou KC (1994) Chem Biol 1: 107

66. Dubois J, Guenard D, Guerittevoegelein F, Guedira N, Potier P, Gillet B, Beloeil JC (1993) Tetrahedron 49: 6533

67. Cachau RE, Gussio R, Beutler JA, Chmurny GN, Hilton BD, Muschik GM, Erickson JW (1994) International Journal of Supercomputer Applications and High Performance Computing 8: 24

68. Boge TC, Himes RH, Vandervelde DG, Georg GI (1994) J Med Chem 37: 3337

69. Ojima I, Kuduk SD, Chakravarty S, Ourevitch M, Begue JP (1997) J Am Chem Soc 119: 5519

70. Georg GI, Harriman GCB, Hepperle M, Clowers JS, VanderVelde DG, Himes RH (1996) J Org Chem 61: 2664

71. Jimenez-Barbero J, Souto AA, Abal M, Barasoain I, Evangelio JA, Acuna AU, Andreu JM, Amat-Guerri F (1998) Bioorg Med Chem 6: 1857

72. Ojima I, Chakravarty S, Inoue T, Lin S, He L, Horwitz SB, Kuduk SD, Danishefsky SJ (1999) Proc Natl Acad Sci U S A 96: 4256

73. Magnani M, Ortuso F, Soro S, Alcaro S, Tramontano A, Botta M (2006) Febs Journal 273: 3301

74. Shanker N, Kingston DGI, Ganesh T, Yang C, Alcaraz AA, Geballe MT, Banerjee A, McGee D, Snyder JP, Bane S (2007) Biochemistry 46: 11514

75. Li YK, Poliks B, Cegelski L, Poliks M, Gryczynski Z, Piszczek G, Jagtap PG, Studelska DR, Kingston DGI, Schaefer J, Bane S (2000) Biochemistry 39: 281

76. Geney R, Sun L, Pera P, Bernacki RJ, Xia SJ, Horwitz SB, Simmerling CL, Ojima I (2005) Chem Biol 12: 339

77. Ojima I, Inoue T, Chakravarty S (1999) J Fluorine Chem 97: 3

78. Paik Y, Yang C, Metaferia B, Tang SB, Bane S, Ravindra R, Shanker N, Alcaraz AA, Johnson SA, Schaefer J, O'Connor RD, Cegelski L, Snyder JP, Kingston DGI (2007) J Am Chem Soc 129: 361

79. Alcaraz AA, Mehta AK, Johnson SA, Snyder JP (2006) J Med Chem 49: 2478

80. Ganesh T, Guza RC, Bane S, Ravindra R, Shanker N, Lakdawala AS, Snyder JP, Kingston DGI (2004) Proc Natl Acad Sci U S A 101: 10006

81. Ganesh T, Yang C, Norris A, Glass T, Bane S, Ravindra R, Banerjee A, Metaferia B, Thomas SL, Giannakakou P, Alcaraz AA, Lakdawala AS, Snyder JP, Kingston DGI (2007) J Med Chem 50: 713

82. Höfle G, Bedorf N, Steinmetz H, Schomburg D, Gerth K, Reichenbach H (1996) Angew Chem Int Ed Engl 35: 1567

83. Taylor RE, Zajicek J (1999) J Org Chem 64: 7224

84. Lange A, Schupp T, Petersen F, Carlomagno T, Baldus M (2007) Chemmedchem 2: 522

85. Carlomagno T, Blommers MJ, Meiler J, Jahnke W, Schupp T, Petersen F, Schinzer D, Altmann KH, Griesinger C (2003) Angew Chem Int Ed Engl 42: 2511

86. Carlomagno T, Sanchez VM, Blommers MJ, Griesinger C (2003) Angew Chem Int Ed Engl 42: 2515

87. Nettles JH, Li H, Cornett B, Krahn JM, Snyder JP, Downing KH (2004) Science 305: 866

88. Reese M, Sanchez-Pedregal VM, Kubicek K, Meiler J, Blommers MJJ, Griesinger C, Carlomagno T (2007) Angew Chem Int Ed Engl 46: 1864

89. Nicolaou KC, Scarpelli R, Bollbuck B, Werschkun B, Pereira MMA, Wartmann M, Altmann KH, Zaharevitz D, Gussio R, Giannakakou P (2000) Chem Biol 7: 593

90. Sanchez-Pedregal VM, Kubicek K, Meiler J, Lyothier I, Paterson I, Carlomagno T (2006) Angew Chem Int Ed Engl 45: 7388

91. Gunasekera SP, Gunasekera M, Longley RE, Schulte GK (1990) J Org Chem 55: 4912

92. Paterson I, Britton R, Delgado O, Meyer A, Poullennec KG (2004) Angew Chem Int Ed Engl 43: 4629

93. Canales A, Matesanz R, Gardner NM, Andreu JM, Paterson I, Diaz JF, Jimenez-Barbero J (2008) Chemistry Submitted

94. Smith AB, 3rd, LaMarche MJ, Falcone-Hindley M (2001) Org Lett 3: 695

95. Monteagudo E, Cicero DO, Cornett B, Myles DC, Snyder JP (2001) J Am Chem Soc 123: 6929

96. Paterson I, Britton R, Delgado O, Wright AE (2004) Chem Commun (Camb): 632

97. West LM, Northcote PT, Battershill CN (2000) J Org Chem 65: 445

98. Liao XB, Wu YS, De Brabander JK (2003) Angew Chem Int Ed Engl 42: 1648

Figure Legends

Figure 1. Electron micrograph of a negatively stained microtubule assembled from purified tubulin and docetaxel. The left side shows the lateral projection of the protofilaments forming a microtubule cylinder ~ 24 nm in diameter which has opened into a sheet on the right side. There are also tubulin oligomers in the image.

Figure 2. Left, cytoplasmic microtubules in interphase kidney epithelial cells imaged with the fluorescent paclitaxel derivative Flutax-2 (green) and nuclear DNA stained with Hoescht 33342 (blue). Right, mitotic spindle from a dividing metaphase cell with similarly imaged microtubules and chromosomes. Bars indicate 10 microns (micrographs courtesy of Isabel Barasoain).

Figure 3.- Polymerization of GTP-Tubulin in 3.4 M Glycerol, 10 mM Sodium Phosphate, 1 mM EGTA, 1 mM GTP, pH 6.7 buffer at 37º C measured by sedimentation. Solid circles: Pelleted tubulin, Hollow circles: tubulin in the supernatant. The critical concentration determined is 5.3 μM; under this total concentration no tubulin is pelleted while over this total concentration all tubulin in excess is pelleted.

Figure 4.- Models of ligand induced tubulin assembly. The ligand induced addition of a tubulin molecule to the microtubule latice is represented. A) Ligand facilitated pathway, a ligand molecule binds to an empty site at the end of a microtubule thus stabilizing the microtubule end. B) Ligand mediated pathway 1. the ligand binds to unassembled tubulin and the ligated dimer has a higher affinity for the microtubules, C) Ligand mediated pathway 2. The binding of a ligand to a non completed site at the end of the microtubule increases the affinity for the binding of the next dimer. Adapted from [32].

Figure 5.- Competition between ^{3}H-paclitaxel and ^{14}C-docetaxel for binding to microtubules. 11.3 μM tubulin was assembled at 37 ºC in PEDTA, 1 mM GDP, 1 mM GTP, 8 mM $MgCl_2$, pH 6.7 by the addition of paclitaxel and docetaxel at a total concentration of 20 μM, at different molar ratios of paclitaxel to docetaxel. The total concentration of microtubules was 11.0 ± 0.10 μM; the concentration of tubulin in supernatants (not polymerized tubulin) varied between ca. 0.4 (in paclitaxel excess) and 0.2 μM (in docetaxel excess). Open circles: ^{3}H-paclitaxel bound per polymerized tubulin dimer; solid circles: ^{14}C-docetaxel bound. Squares: total ligand (paclitaxel plus docetaxel) bound per polymerized tubulin dimer. The solid lines are the best fit to the data, employing a simple competition model of the two ligands for the same site, taken from [34].

Figure 6.- Scheme of the structures of epothilone analogues studied in [35], the chemical differences between them, and the effect of these modifications in the free energy of binding to their site in microtubules at 35 °C. Taken from [35]

Figure 7.- Kinetics of binding of Flutax1 to microtubules at 35°C. In the stopped-flow device a 1 mM solution of Flutax1 was mixed with 25 mM pure tubulin assembled into microtubules (concentration of sites 20 mM) (final concentrations of 500 nM Flutax and 10 mM sites) in the absence (a) and presence (b) of 50 mM docetaxel. Curve a is fitted to an exponential decay. Inset: Residues between the experimental and theoretical curves. Taken from [10].

Figure 8.- Insight of the outer (A) and (B) inner surface of a high resolution microtubule model, showing two different types of pores, I and II (see text). Green beads, polar residues; yellow beads, hydrophobic residues; red beads, acid residues; blue beads, basic residues; white beads, paclitaxel bound at its

site, grey beads, nucleotide. (C) Detail of a type I pore viewed from above. Ribbon representation of two neighbour β-tubulin subunits as seen from the plus end of the microtubule, paclitaxel, GDP and the four residues forming a putative taxoid binding site are shown in Van der Waals representation. Taken from [22].

Figure 9.- (A) Model for the binding of cyclostreptin at the proposed initial MSA binding site at pore type I. Taken from [21]. (B) Scheme of the route of paclitaxel to its lumenal site in the microtubules. Paclitaxel binds to the external site at the pores of the microtubules, being later transported to its lumenal site while the external site gets blocked. In the presence of cyclostreptin the external site gets irreversibly blocked; thus, paclitaxel can not reach the lumenal site.

Figure 10. The X-ray structure of docetaxel [56].

Figure 11. The polar conformer of paclitaxel.

Figure 12. The T-Taxol conformer.

Figure 13. Superimposition of the X-ray structure of discodermolide (black) [91], bound to non-assembled tubulin (blue) [90] and bound to microtubules [93]. Minor adjustments are observed.

Figure 14A. Superimposition of the bound conformers of discodermolide and dictyostatin bound to assembled microtubules [93]. 14B. The AUTODOCK solution of discodermolide and dictyostatin (blue) bound to tubulin (1JFF), also compared with bound paclitaxel (green).

Figure. 15. Superimposition of the two major conformers of Peluroside A coexisting in water solution [26].

Tables

Table I.- Kinetic rates of taxane site ligands binding to microtubules. 37 ºC

	k_{+1} x$10^5 M^{-1}s^{-1}$	k_{-1}	k_{+2}	k_{-2} s^{-1}
Flutax-1[a]	6.10±0.22	0.99±0.27	0.0243±0.0007	0.026±0.0012
Flutax-2[a]	13.83±0.18	1.63±0.18	2.7±0.8	0.022±0.0012
Paclitaxel[b]	3.63±0.08	ND	ND	0.091±0.0061
Epothilone A[c]	3.3±0.03	ND	ND	0.138±0.37(slow) 0.463±0.32(fast)

[a]Data from [10]
[b]Data from [22]
[c]Data from [42]

Table 2.- Kinetic rates of epothilone A dissociation[a]

	25ºC	30ºC	35ºC	37ºC	40ºC
Kfast	ND	ND	0.445	0.463	0.635
Afast	ND	ND	0.25	0.35	0.38
Kslow	0.020	0.052	0.126	0.138	0.199
Aslow	1	1	0.74	0.65	0.62

[a] Determined for this work as described in [42].

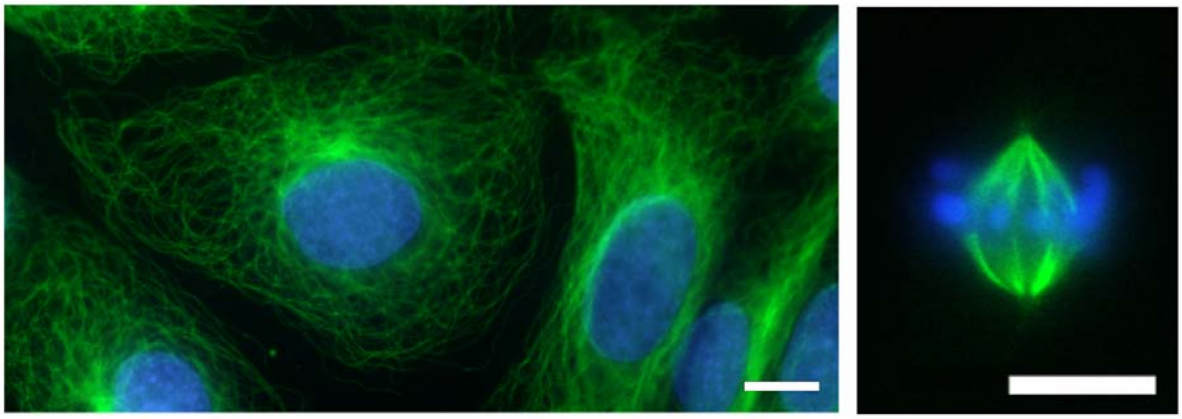

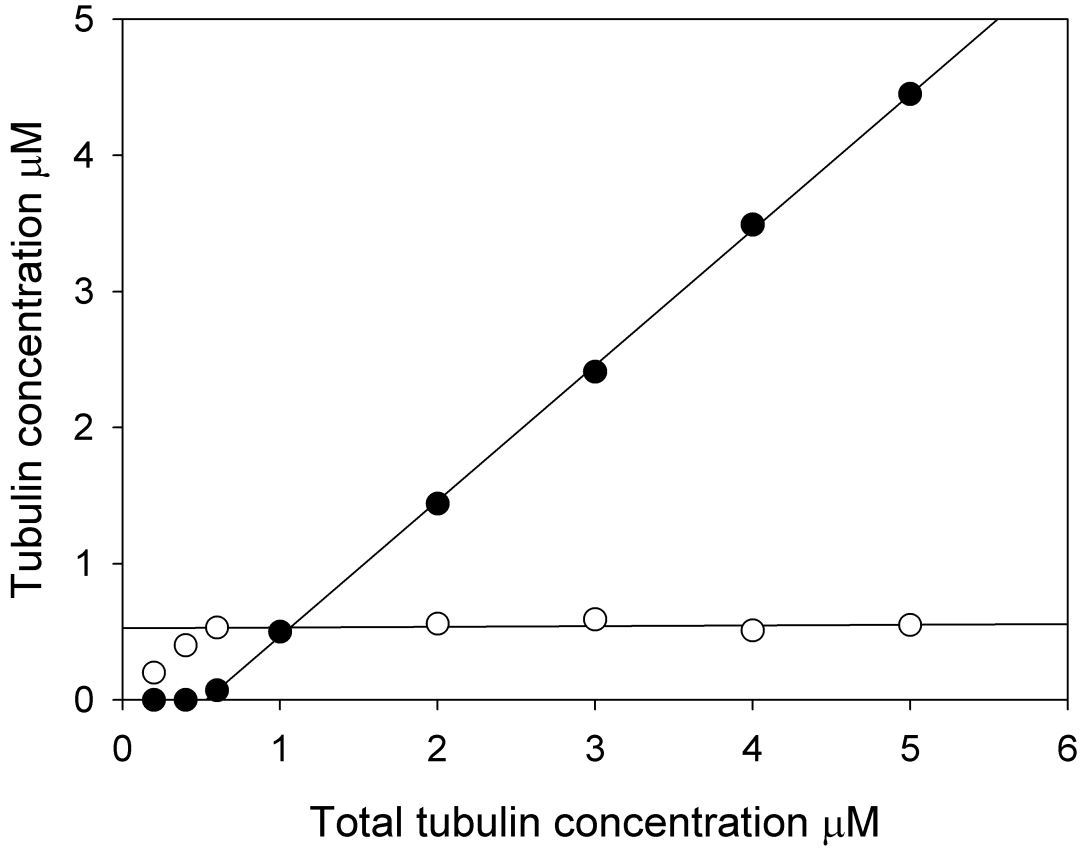
Tubulin concentration μM
Total tubulin concentration μM
0
1
2
3
4
5
6

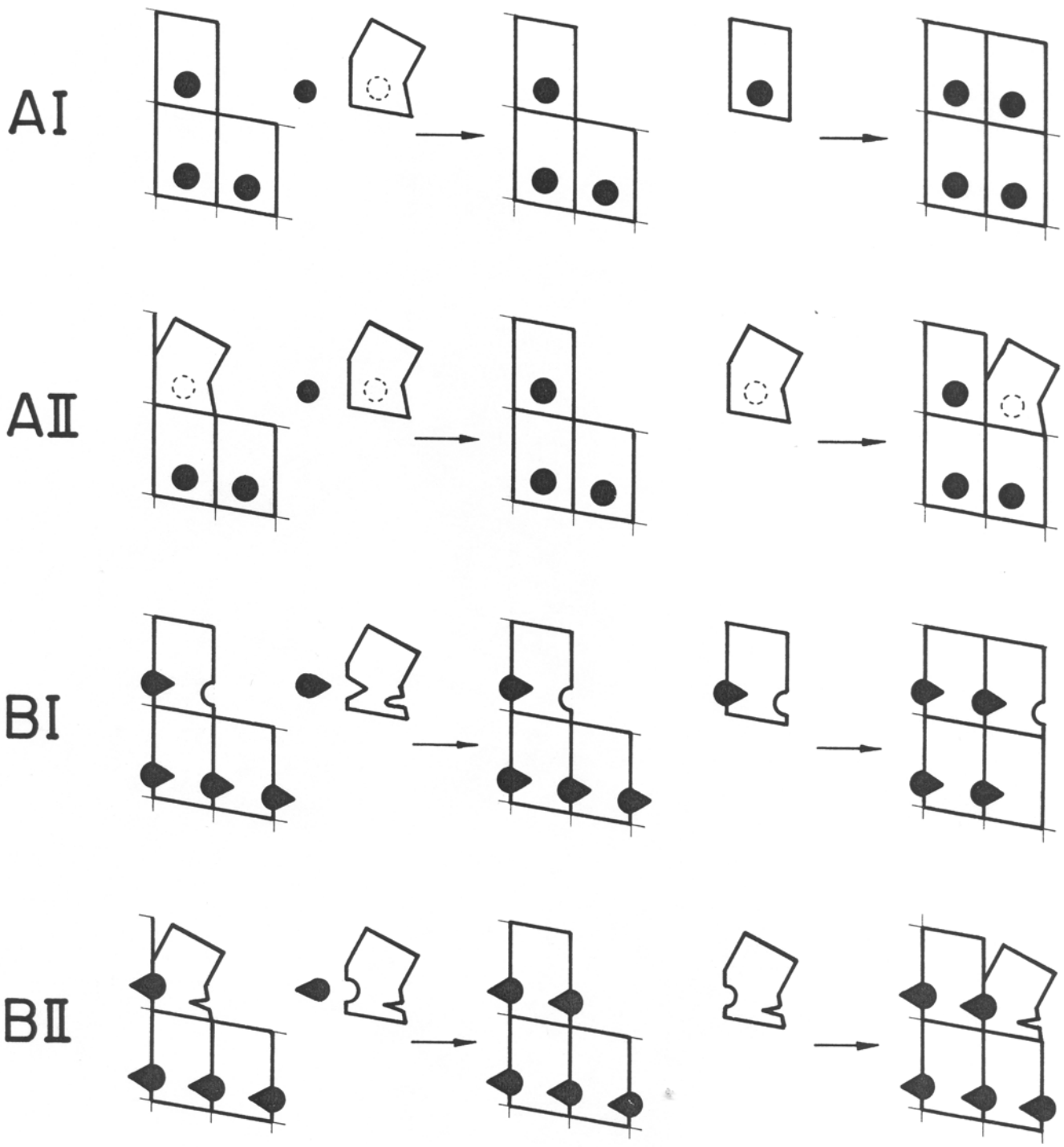
AI
AII
BI
BII

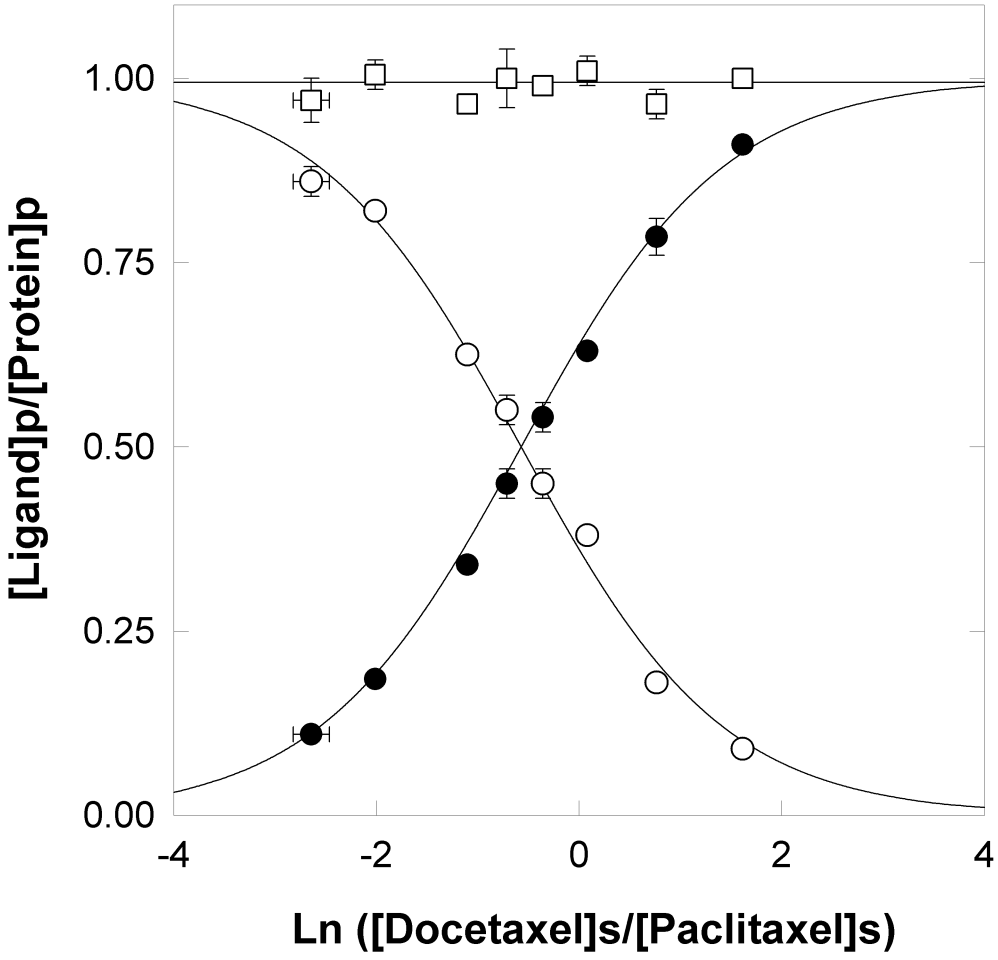
1.00
0.75
0.50
0.25
0.00
-4
-2
0
2
4
[Ligand]p/[Protein]p
Ln ([Docetaxel]s/[Paclitaxel]s)

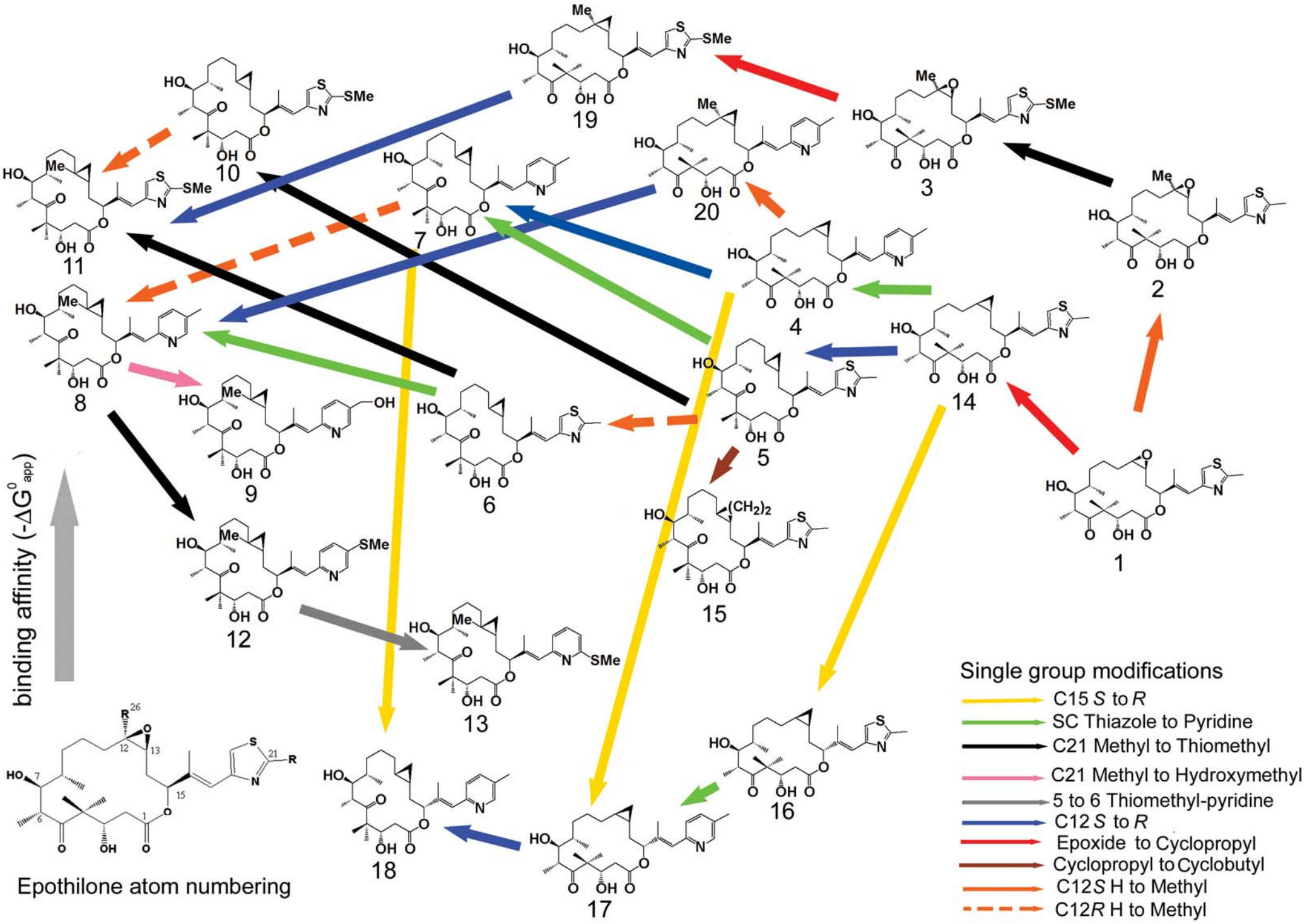
binding affinity ($-\Delta G^0_{app}$)
Epothilone atom numbering
Single group modifications
C15 S to R
SC Thiazole to Pyridine
C21 Methyl to Thiomethyl
C21 Methyl to Hydroxymethyl
5 to 6 Thiomethyl-pyridine
C12 S to R
Epoxide to Cyclopropyl
Cyclopropyl to Cyclobutyl
C12S H to Methyl
C12R H to Methyl

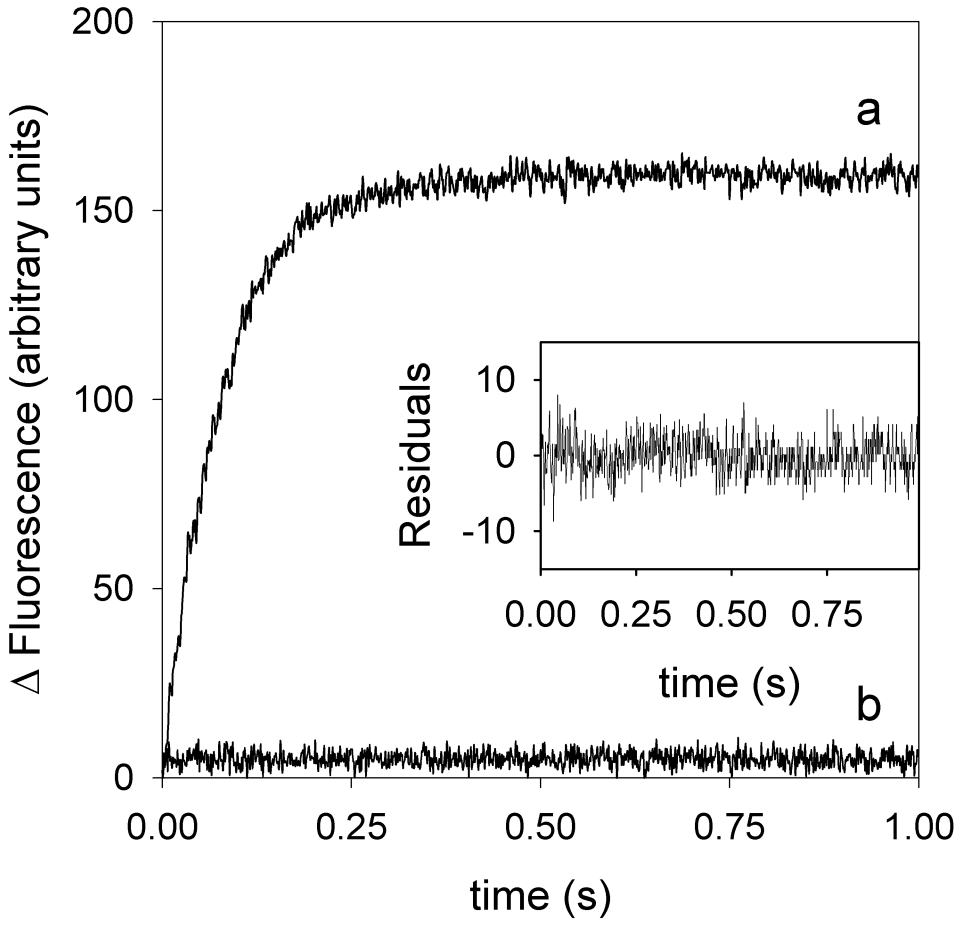
200
150
100
50
0
Δ Fluorescence (arbitrary units)
a
b
0.00
0.25
0.50
0.75
1.00
time (s)
Residuals
10
0
-10
0.00
0.25
0.50
0.75
time (s)

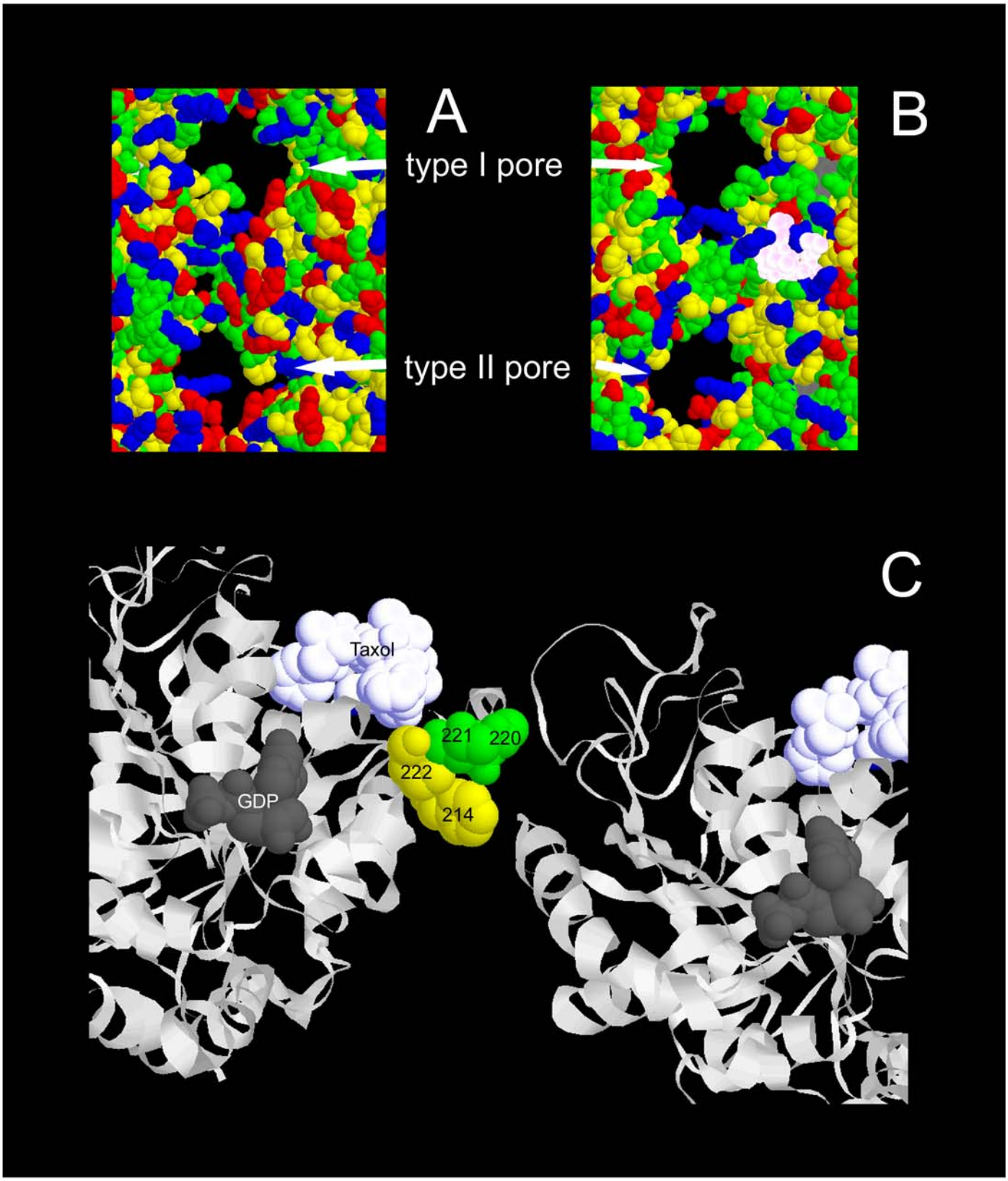
A
type I pore
type II pore
B
C
Taxol
GDP
221
220
222
214

A

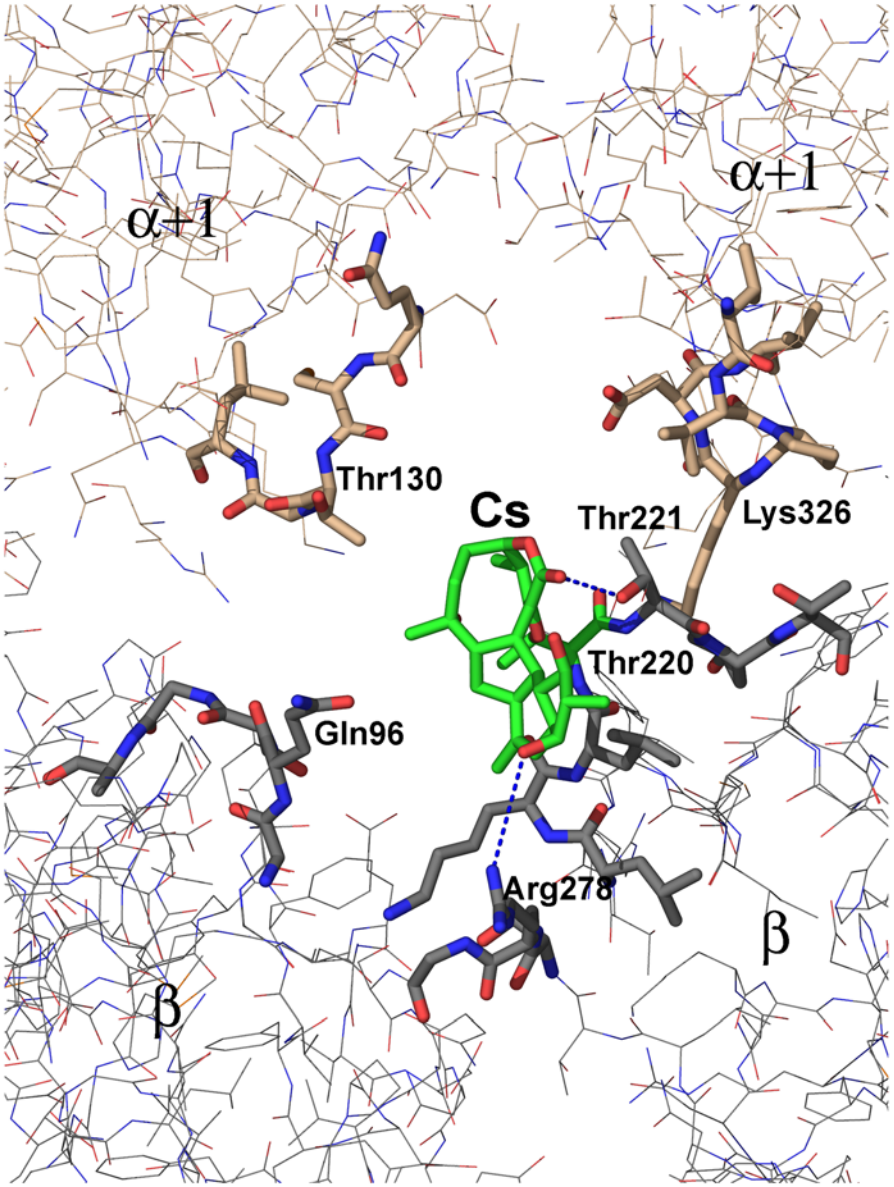
α+1
α+1
Thr130
Cs
Thr221
Lys326
Thr220
Gln96
Arg278
β
β

minus end

B

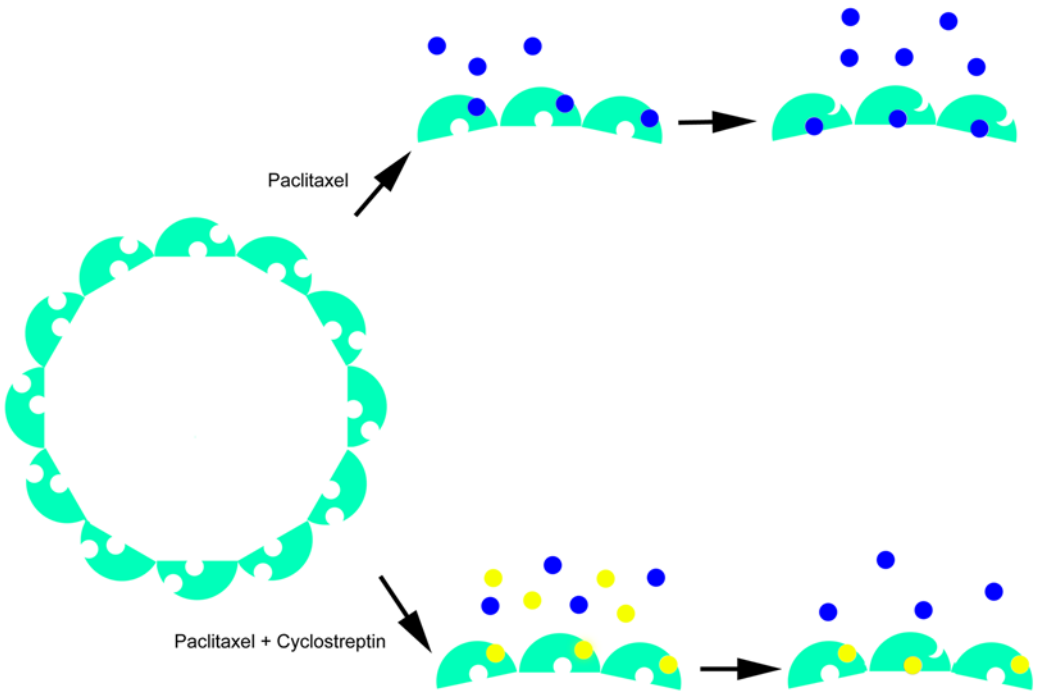
Paclitaxel
Paclitaxel + Cyclostreptin

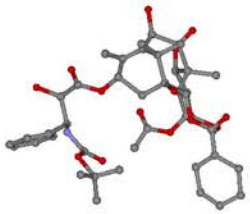

Figure 10

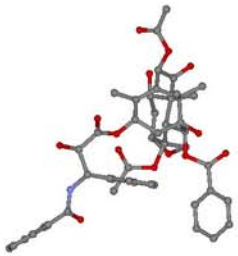

Figure 11

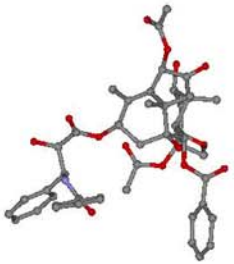

Figure 12

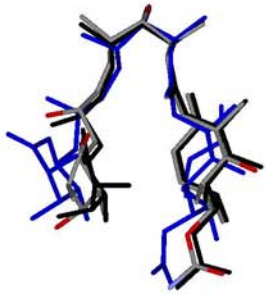

Figure 13

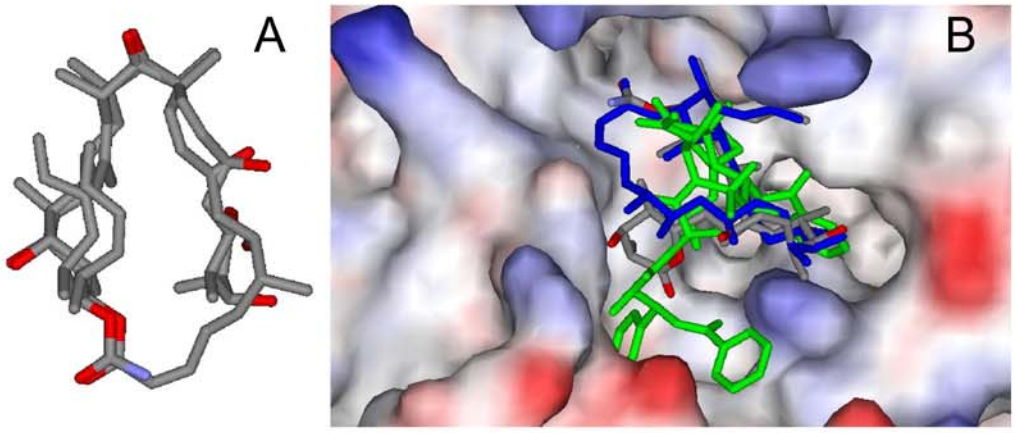

Figure 14

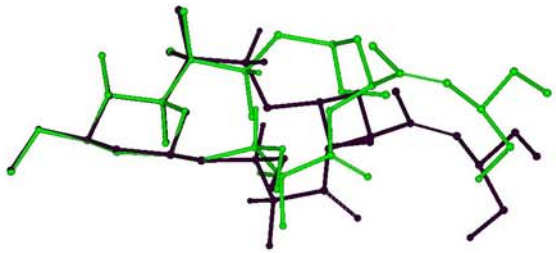

Figure 15